Signal, Image and Video Processing (2020) 14:1555–1563
https://doi.org/10.1007/s11760-020-01695-3

ORIGINAL PAPER

Restoration of highly salt-and-pepper-noise-corrupted images using novel adaptive trimmed median filter

Bharat Garg[1]

Received: 20 July 2019 / Revised: 1 March 2020 / Accepted: 17 April 2020 / Published online: 16 May 2020

Abstract

The paper presents a novel adaptive trimmed median (ATM) filter to remove salt-and-pepper (SAP) noise of high noise density (ND). The proposed filter computes median of trimmed window of adaptive size containing noise-free pixels (NFP) for ND up medium range while performs new interpolation-based procedure at high ND. Further, for the rare scenarios especially at the boundary where denoising using interpolation is not good enough, the proposed filter denoises the candidate pixel with the help of nearest processed pixels. The proposed ATM filter effectively suppresses SAP noise because denoising mostly utilizes original non-noisy pixels. The proposed algorithm is evaluated for varying ND (10–90%) with different benchmark images (greyscale and coloured) over the existing approaches. The proposed ATM filter on an average provides 1.59 dB and 0.37 dB higher PSNR values on the greyscale and color images, respectively.

Keywords Median filter · Interpolation · Salt-and-pepper noise · Image processing

1 Introduction

The images are inevitably contaminated by the impulse noise during image acquisition, transmission and/or storage due to malfunctioning of camera sensors, noise in transmission channel and/or fault in memory, respectively. In the impulse noise, salt-and-pepper (SAP) noise significantly degrades image quality; therefore, nonlinear filters are presented to retrieve the noise-free image. Among the several nonlinear filters, the median filter (MF) is more popular for the removal of SAP noise without destroying image information. However, the standard MF (SMF) is only able to recover image corrupted with low noise density (ND) [1]. At higher ND ($ND > 50\%$), the SMF does not get sufficient noise-free pixels (NFPs) within local window to restore noisy-pixel and therefore fails to recover original image.

The adaptive MF (AMF) [2] increases the window size with ND to remove corrupted pixel. However, it exhibits blurring effects at higher noise density. The modified switching MFs [3,4] take decision on the noisy pixel on the basis of the pre-defined threshold. The prime limitation of these filters is the implementation of method that provides correct decision. An improved tolerance-based selective arithmetic mean (ITSAM) filter [5] detects the ND, and if it is found above a given threshold, it restores noisy-pixel by the mean of current window (CW), else leaves the pixel unaltered by considering it as NFP. A decision-based algorithm for median (DBAM) filter [6] performs the sorting in CW horizontally, vertically and diagonally and takes the centre pixel as denoised pixel. If the pixel is still noisy, the algorithm restores the pixel by previously processed pixel.

An iterative adaptive alpha-trimmed mean (IAATM) filter [7] restores noisy pixels via a fuzzy detection followed by a weighted mean operation. Since IAATM restores noisy pixel by the median of trimmed window or mean of CW when it has noisy pixels only, it provides good image quality. A modified decision-based unsymmetric trimmed median (MDBUTM) filter restores the noisy pixel by median of NFPs if available in CW or by mean value of all noisy pixels [8]. Although the MDBUTM provides improved image quality, consideration of noisy pixels to restore candidate pixel provides large error at higher noise density. Further, some improved MDBUTM algorithms are presented in [9,10].

A modified direction weighted (MDW) filter [11] first estimates the ND in the local window and then computes weighted mean of the recursive or non-recursive window based on the computed ND for denoising. An adaptive weighted mean filter [12] first determines appropriate win-

✉ Bharat Garg
bharat.garg@thapar.edu

[1] Thapar Institute of Engineering and Technology, Patiala, India

dow by increasing its size until the minimum and maximum values of two consecutive windows are equal, respectively, and then replaces noisy pixel by the weighted mean of CW, whereas NFPs remain unaltered. A fast switching-based median-mean (FSBMM) filter [13] denoises corrupted pixel by the median of CW. If the result of median is noisy, the candidate noisy-pixel is restored by the nearest neighbour processed pixel. Further, if the corrupted pixel is first pixel or belongs to the first row or first column of the image, then it is restored by the mean of CW, previously processed pixel of upper row or left column, respectively.

An adaptive switching weighted median (ASWM) filter [14] first classifies pixel as noisy or noise-free and then denoises by the median of adaptive weighted window. Further, a recursive cubic spline interpolation (RSI) filter algorithm is presented in [15] for the high-density SAP noise removal, whereas a local and global image information-based filter estimates ND and then denoises based on block-level and global image information [16]. Due to the consideration of global information, it improves the quality of denoised images.

A direction weighted median (DWM) filter [17] computes weighted sum of absolute difference in four directions to identify the current pixel to be noisy or noise-free. Further, weighted median in the direction exhibiting closely related pixels restores the noisy pixel. The DWM filter iteratively applies detection process with decreasing threshold to improve detection accuracy which leads to high computational complexity. A modified DWM filter [18] considers 7×7 window and detects pixel to be either noisy, noise-free or edge pixel in 12 directions to improve detection efficiency. Further, an extension of the DWM filter is presented in [19] where different window size is selected based on ND. A mixed noise removal (MNR) algorithm [20] uses adaptive directional weighted mean filter and improved adaptive anisotropic diffusion model to remove impulsive noise and Gaussian noise, respectively. The MNR algorithm first classifies all pixels as noisy-pixels corrupted by either impulse noise or Gaussian noise and then restores using adaptive directional weighted mean filter or adaptive anisotropic diffusion, respectively.

An adaptive fuzzy inference system (AFIS)-based DMF (AFIS-DMF) [21] first creates fuzzy membership function and then accurately classifies pixel as noisy (labelled differently when belongs to smooth or edge regions) or noisy-free. Finally, the noisy pixels under smooth and non-smooth regions are restored by median and directional median filters, respectively. The fuzzy directional median (FDM) filter [22] improves the detection accuracy by first discriminating smooth and non-smooth regions and then detecting noisy pixels in these regions differently. Further, removal of noisy pixels is done in smooth and non-smooth regions using median of 3×3 window and directional median of the pixels aligning with the direction of smallest standard deviation, respectively. However, FDM filter is effective for the removal of impulse noise up to 30% ND. A color edge detector robust to impulsive and Gaussian noise using anisotropic morphological directional derivative and singular value decomposition is presented in [23].

Algorithm 1 ATM(Img, $OutImg$)

```
Input Img: Input Image
Output OutImg: Output Image
for each pixel iP_{i,j} of Img do
    Set flag (f_{i,j}) value to 1, if non-noisy else to 0.
    if f_{i,j} == 1 then
        oP_{i,j} ← iP_{i,j};
    else
        Compute n_{nfp};                              ▷ Compute n_{nfp} in window w_{3x3}
        if n_{nfp} > n_{cw}/l_{cw} then
            oP_{i,j} ← median(w_{cnf});
        else
            Increase current window size to 5 × 5
            Compute n_{nfp};                          ▷ Compute n_{nfp} in w_{5x5}
            if n_{nfp} > n_{cw}/l_{cw} then
                oP_{i,j} ← median(w_{cnf});
            else
                [fi, pix] ← PIT(w_{3x3})              ▷ Call PIT procedure
                if fi == 1 then
                    oP_{i,j} ← pix;
                else
                    oP_{i,j} ← PPR(w_{3x3});
                end if
            end if
        end if
    end if
    OutImg(i, j) =← oP_{i,j};
end for
Return OutImg;
Procedure: PIT(w_{3x3})                               ▷ Proposed interpolation procedure
if (f_{1,1} == 1)&&(f_{3,3} == 1) then
    fi ← 0; pix ← (w_{1,1} + w_{3,3})/2;
else if (f_{1,3} == 1)&&(f_{3,1} == 1) then
    fi ← 0; pix ← (w_{1,3} + w_{3,1})/2;
else if (f_{2,1} == 1)&&(f_{2,3} == 1) then
    fi ← 0; pix ← (w_{2,1} + w_{2,3})/2;
else if (f_{1,2} == 1)&&(f_{3,2} == 1) then
    fi ← 0; pix ← (w_{1,2} + w_{3,2})/2;
else if ((f_{1,1}==1)||(f_{1,3}==1))&&((f_{3,1}==1)||(f_{3,3}==1)) then
    fi ← 0; pix ← mean(w_{1,1} + w_{1,3} + w_{3,1} + w_{3,3});
else
    fi ← 1;
end if
Return [fi, pix];
Procedure: PPR(w_{3x3})                               ▷ Nearest processed pixel procedure
if ((i == 1)&&(j == 1))||((i == R)&&(j == C)) then
    pix ←median(w_{cnf});
else if ((i == 1)||(i == R)) then
    pix ← oP_{i,j−1}
else if ((j == 1)||(j == R)) then
    pix ← oP_{i−1,j}
else
    pix ← mean(oP_{i,j−1}, oP_{i−1,j−1}, oP_{i−1,j}, oP_{i−1,j+1})
end if
Return pix;
```

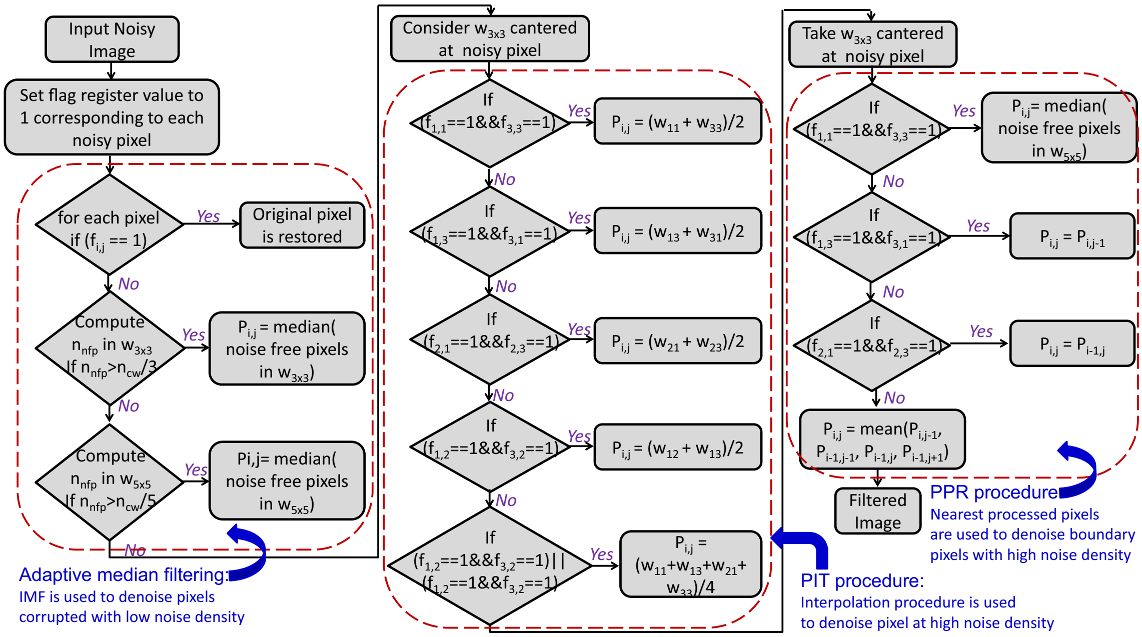

Fig. 1 Flow chart showing various steps of the proposed ATM filtering approach

Recently, a convolutional neural network (CNN) with the multi-layer structure for SAP noise removal is presented in [24]. It generalizes the applications of deep learning for SAP noise removal. A non-local switching filter CNN (NLSF-CNN) algorithm is presented in [25] which consists of two steps, namely NLSF processing and CNN training steps. The preprocessing step reduces the interference of high-intensity noise in deep learning process and yields high-quality denoised images.

Recently, a probabilistic decision-based (PDB) filter is presented in [26]. The PDB filter estimates the denoised pixel by either trimmed median (TM) [8] or patch median (PM) [6] based on the noise density. A three-value weighted approach (TVWA) [27] computes maximum, minimum and middle values from the local window, and if not found, the window size is increased. In TVWA, the NFPs of CW are segmented into three groups based on their closeness to minimum, maximum and middle value. The weight of each group is determined by the number of NFPs in that group over the total number of NFPs in the CW. Finally, the denoised pixel is evaluated by the summing of these values multiplied by their weights. However, it shows poor PSNR value at very high ND ($> 80\%$). An linear prediction-based adaptive MF first decides the pixel to be noisy based on a threshold and then denoises using median of adaptive window [28]. In [29], a different applied MF (DAMF) is presented that considers value of neighbour pixels and adaptive window to remove SAP noise. Recently, a based on pixel density filter (BPDF) [30] that first determines whether current pixel is noisy or noise-free and then decides adaptive window size where most repetitive NFP restores the noisy pixel.

Based on the above observations, denoising at high ND ($> 60\%$) while maintaining the image details is a very challenging task. Therefore, this paper introduces a novel adaptive trimmed median (ATM) filter that denoises the image using median of NFPs of adaptive CW. At excessive ND, on the basis of number of NFPs, the proposed filter reconstructs the pixel either using novel interpolation approach or mean of previously processed pixels. The proposed filter efficiently eliminates the SAP noise while maintains the edge details and image information. The simulation results show superior PSNR and SSIM values by the proposed ATM filter over the advanced SAP removal techniques.

The paper is organized as follows: Sect. 2 presents proposed ATM algorithm with its flow chart, whereas Sect. 3 shows an illustration of denoising using the proposed algorithm. Section 4 presents simulation results and analysis on various benchmark images with varying ND. Finally in Sect. 5, conclusions are drawn.

2 Proposed ATM filter algorithm

The proposed ATM algorithm initially examines the current pixel to be processed is noisy or noise-free. If the candidate pixel is noisy, median of NFPs of the CW is estimated when the noise density is low and middle range, whereas at high noise density the proposed ATM filter utilizes the proposed interpolation technique (PIT) or previously processed pixels

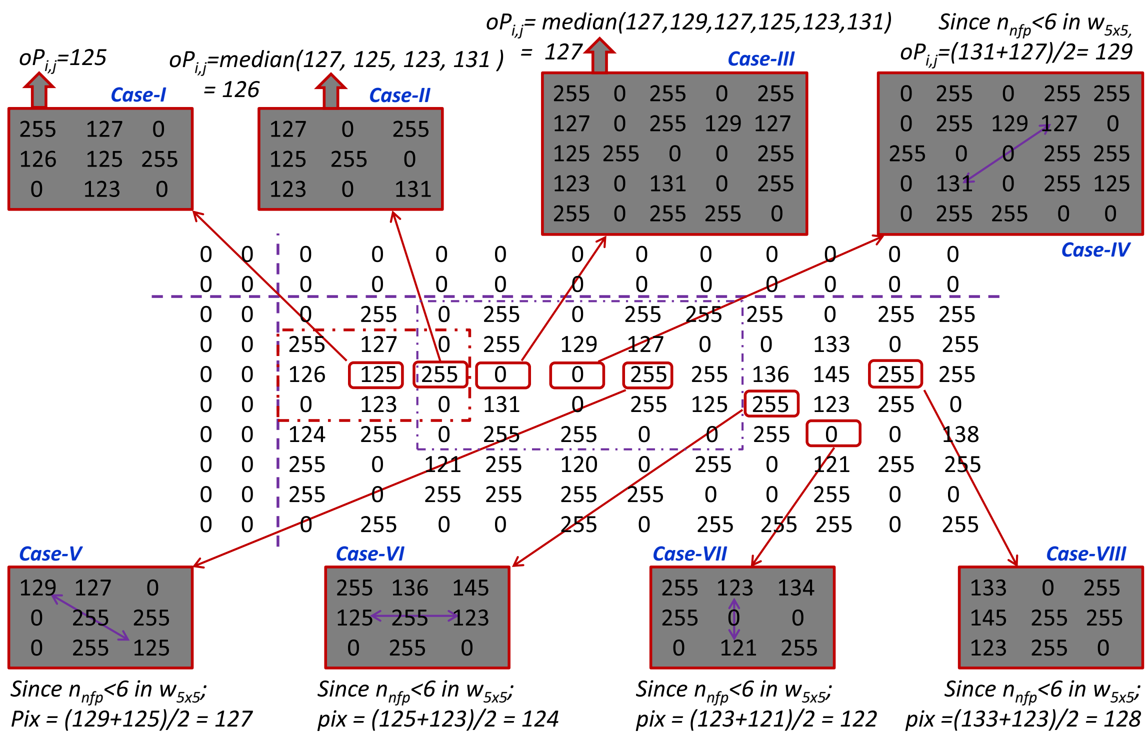

Fig. 2 An illustration showing examples to estimate denoised pixels using proposed ATM algorithm

replacement (PPR) procedure to denoise the candidate pixel. The pseudo codes of the proposed algorithm are given in Algorithm 1 where, Img and $OutImg$ are the input (noisy) and output (filtered) images, respectively. In the proposed algorithm, initially, a flag ($f_{i,j}$) corresponding to the current input pixels ($iP_{i,j}$) is set to 1 if it is noise-free, otherwise set to 0. The $oP_{i,j}$, n_{cw}, l_{cw}, n_{nfp}, w_{3x3} and w_{cnf} represent filtered pixel, number of pixels in the CW (w_c), length of w_c, number of NFPs in w_c, window of size 3×3 and the current window after removal of noisy pixels, respectively.

The proposed algorithm denoises image by initially considering 3×3 sliding window centred at the candidate pixel. If the centred pixel ($iP_{i,j}$) is noise-free, it is left unaltered otherwise flag register for the CW is computed. Further, the number of NFPs (n_{nfp}) in the CW is computed and if found more than n_{cw}/l_{cw}, the denoised pixel is computed by the median of w_{cnf}; otherwise, window size is increased to 5×5. Similar to the 3×3 window, n_{nfp} in the current 5×5 window is computed, and if it is found greater than n_{cw}/l_{cw}, the median w_{cnf} is assigned as denoised pixel. If the above conditions fail, it represents high noise density and therefore requires more intelligent operations to compute denoised value. In the case of high noise density (when $n_{nfp} \leq n_{cw}/l_{cw}$), the proposed algorithm calls the interpolation procedure or replacement by the previously processed pixels procedure to compute denoised pixel.

In the proposed interpolation procedure, 3×3 window is considered and denoised pixel is computed by the bilinear interpolation in either first diagonal, second diagonal, horizontal line passing through candidate noisy pixel or the vertical line passing through the candidate noisy pixel based on the availability of NFPs in the corresponding locations. For example, to estimate the denoised value using first diagonal, both corner pixels of current window ($w_{1,1}$ and $w_{3,3}$) must be noise free; otherwise, it will go to second diagonal. If the NFPs are not found in second diagonal also, then it computes denoised pixel based on the availability of NFPs in either row or column passing through candidate noisy pixel. Finally, it checks at least one NFP at the top two corners and at least one NFP at the bottom two corners. If the algorithm finds the NFPs, then denoised pixels are estimated as the mean of all corner pixels. If the interpolation procedure is unable to reconstruct the denoised pixel, then PPR procedure is called. The PPR procedure denoises the candidate pixel by the median of w_{cnf}, previously processed in the same row, previously processed pixel in the same column or mean of nearest four already processed pixels if the candidate pixel belongs to the first pixel, first row, first column, or all pixels except first row and column of the image, respectively.

The proposed algorithm is illustrated by the flow chart as shown in Fig. 1. The flow chart is segmented in to three sections encircled by three rectangles with rounded corners. The first rectangle denoises the pixel by the median of window size changes from 3×3 to 5×5 based on the ND. It provides valid denoised pixel if the noise density is low and median ranges. At the high noise density, the second rectangle is

Table 1 Average PSNR, SSIM and computation time of proposed ATM and existing SAP removal techniques using different benchmark images with varying noise density

Metrics	ND (%)	SMF [1]	DBAM [6]	ITSAM [5]	MDBUTM [8]	FSBMM [13]	RSI [15]	PBDM [26]	DAMF [29]	BPDM [30]	Prop. ATM
(PSNR (dB)	10	27.12	33.71	30.88	28.20	34.66	34.87	24.36	28.22	22.70	36.00
	20	24.45	27.50	29.37	27.77	31.18	31.11	19.55	27.80	19.69	32.85
	30	21.10	22.99	28.50	27.06	28.74	29.07	16.90	27.08	17.89	30.50
	40	17.35	18.59	27.14	26.33	27.02	27.05	15.36	25.88	16.54	28.67
	50	14.22	15.29	25.29	25.46	25.29	25.65	14.51	25.47	15.52	27.22
	60	11.52	12.48	23.32	24.17	24.40	24.52	13.64	24.17	14.41	26.24
	70	9.37	10.21	20.66	21.56	23.38	22.86	12.71	21.52	13.46	24.92
	80	7.68	8.24	17.16	18.45	22.11	21.13	11.19	18.44	12.22	23.18
	90	5.76	6.69	12.08	14.99	19.57	18.40	8.55	14.98	10.04	21.04
	Avg	15.40	17.30	23.82	23.78	26.26	26.07	15.20	23.73	15.83	27.85
SSIM	10	0.8551	0.9699	0.9127	0.8313	0.9335	0.9318	0.8475	0.8313	0.6397	0.9757
	20	0.8054	0.9123	0.9026	0.8249	0.9121	0.9074	0.6078	0.8249	0.4894	0.9491
	30	0.6799	0.7968	0.8807	0.8133	0.8853	0.8836	0.4106	0.8133	0.3902	0.9302
	40	0.4713	0.5744	0.8362	0.7991	0.8541	0.8531	0.3011	0.7991	0.3368	0.9065
	50	0.2658	0.3563	0.7511	0.7768	0.8146	0.8205	0.2415	0.7768	0.2865	0.8796
	60	0.1366	0.2113	0.6451	0.7211	0.7788	0.7816	0.1925	0.7211	0.2430	0.8502
	70	0.0646	0.1259	0.5216	0.5873	0.7384	0.7242	0.1544	0.5873	0.1949	0.8110
	80	0.0316	0.0663	0.3755	0.3919	0.6862	0.6472	0.1142	0.3919	0.1289	0.7513
	90	0.0154	0.0295	0.1999	0.1910	0.5884	0.5073	0.0562	0.1910	0.0608	0.6306
	Avg	0.3695	0.4492	0.6695	0.6596	0.7990	0.7841	0.3251	0.6596	0.3078	0.8538
Computation time (s)	10	0.052	0.029	0.630	0.349	0.041	1.472	0.024	0.441	0.672	0.042
	20	0.088	0.046	0.726	0.352	0.075	2.943	0.049	0.495	1.379	0.075
	30	0.138	0.072	0.740	0.355	0.109	4.576	0.084	0.531	2.033	0.120
	40	0.166	0.092	0.863	0.410	0.124	5.324	0.123	0.592	2.940	0.145
	50	0.212	0.133	0.942	0.412	0.158	7.154	0.192	0.696	4.404	0.173
	60	0.261	0.170	0.975	0.437	0.184	9.639	0.287	0.783	5.943	0.198
	70	0.318	0.232	1.027	0.450	0.202	12.142	0.414	0.904	7.119	0.222
	80	0.380	0.302	1.117	0.474	0.242	16.322	0.572	1.015	8.122	0.263
	90	0.447	0.385	1.154	0.495	0.297	20.628	0.810	1.182	9.528	0.315
	Avg	0.229	0.162	0.908	0.415	0.159	8.911	0.284	0.738	4.682	0.173

called-off and estimates denoised pixel using the proposed interpolation technique. At very high noise density or for pixels belonging to the boundary of the image, replacement by the previously processed pixels procedure is called as shown by third rectangle. The next section presents an illustration of the proposed approach using an example.

3 Illustration of proposed algorithm

The estimation of denoised pixel using the proposed algorithm with the help of few examples is demonstrated in Fig 2. Since the current pixel to be processed is noise-free (as shown by the first shaded rectangle at the top left corner, *Case-I*), it is left unaltered, *i.e*. output pixel is equal to input pixel ($oP_{i,j} = iP_{i,j} = 125$). At low noise density, when ($n_{nfp} > n_{cw}/3$) median of w_{cnf} is employed to estimate NFPs [$oP_{i,j} = median(127, 125, 123, 131) = 126$]. The computed pixel is shown by the second rectangle (*Case-II*) from left rectangle at top. Similarly, at some more noise density, window size of 5×5 is used to estimate denoised pixel (*Case-III*). At very high noise density, where the number of NFPs (n_{nfp}) is very small ($n_{nfp} \leq n_{cw}/l_{cw}$) in the current window (w_c), interpolation procedure is called. The PIT procedure first checks the availability of NFPs in the first diagonal if current window (3×3 size). The PIT procedure then replaces candidate noisy pixel by the mean of these two corner pixels as shown by the top right corner rectangle (*Case-IV*). Similarly, the estimation of denoised pixel for other conditions is also illustrated in Fig. 2 (*Case-V–Case-VIII*). The next section presents a comparative analysis of proposed ATM algorithm over the existing.

4 Simulation results and analysis

The efficacy of proposed ATM approach is analysed over the existing techniques, namely SMF [1], DBAM [6], ITSAM [5], MDBUTM [8], FSBMM [13], RSI [15], PDBM [26], DAMF [29] and BPDM [30] using different benchmark images. The quality metrics such as peak-signal-to-noise ratio (PSNR) and structural similarity index (SSIM) [31] are extracted. Both quantitative and qualitative analyses are done based on the extracted quality metrics and reconstructed images, respectively. This section first presents the average quality metrics and run-time of proposed and existing filters using different benchmarks images having noise densities varied from 10% to 90%. Finally, the performance analysis on the color images (Lena and Mandrill) is presented.

The average quality metrics and run time of the proposed and existing filters using different benchmark images (Cameraman, House, Jetplane, Lake, Mandrill, Peppers, Pirate and Walkingbridge) with noise density varied from 10–90% are summarised in Table 1. The simulation results show that the proposed ATM filter on an average yields higher PSNR value over all the existing algorithms even at higher noise density. Similarly, it can also be seen that the proposed ATM filter provides superior SSIM metrics in comparison with the existing algorithm at each noise density level. However, the computation time of the proposed filter is little more than that of the DBAM [6] and FSBMM [13] filters. The proposed filter provides higher value of quality metrics over these filters. Finally, the comparison of PSNR and SSIM with varying noise density is illustrated by the plots shown in Fig. 3. The higher SSIM by the proposed ATM algorithm displays superior restoration of image contents.

The extracted images are shown in Fig. 4 for the qualitative exploration of proposed filter. It can be seen from the reconstructed images that the images with large edges (e.g. Mandrill) exhibit smaller value of quality, while the images with less edges contents (e.g. Cameraman) have higher value. However, whatever the image is, the proposed filter provides a higher visual quality over the existing one as shown in Fig. 4j.

Finally, the efficacy of proposed filter is also evaluated on color images (Lena and Mandrill images (256×256 size) are considered). The SAP noise with 90% noise density is first introduced and then filtered by the proposed and existing filters. The extracted quality metrics are shown in Table 2 for the quantitative comparison. The simulation results show that proposed MF provides higher value of PSNR and SSIM over the existing filters for each benchmark images. On an average, the proposed filter provides 0.37 dB and 0.0177 higher PSNR and SSIM metrics, respectively. For the qualitative comparison, the processed images (Lena and Mandrill images) using proposed and existing filters are shown in Fig. 5. The figure shows that the quality of images restored using proposed filter is superior over the images restored using existing filters.

5 Conclusion

This paper presents a novel SAP noise removal algorithm that effectively restores noisy pixel using either median of adaptive window size or proposed interpolation technique based on the noise density. Further, at high noise density, the proposed ATM filter provides fine estimation of noisy pixel available on the boundary by the replacement using the nearest processed pixels procedure. The proposed ATM algorithm is evaluated over the different benchmark images with varying noise density (10–90%). The extracted quality metrics show that the proposed filter on an average provides 1.59 dB and 0.0548 higher PSNR and SSIM values, respectively, on the greyscale images, while 0.37 dB and 0.0177 higher values of PSNR and SSIM, respectively, on the color

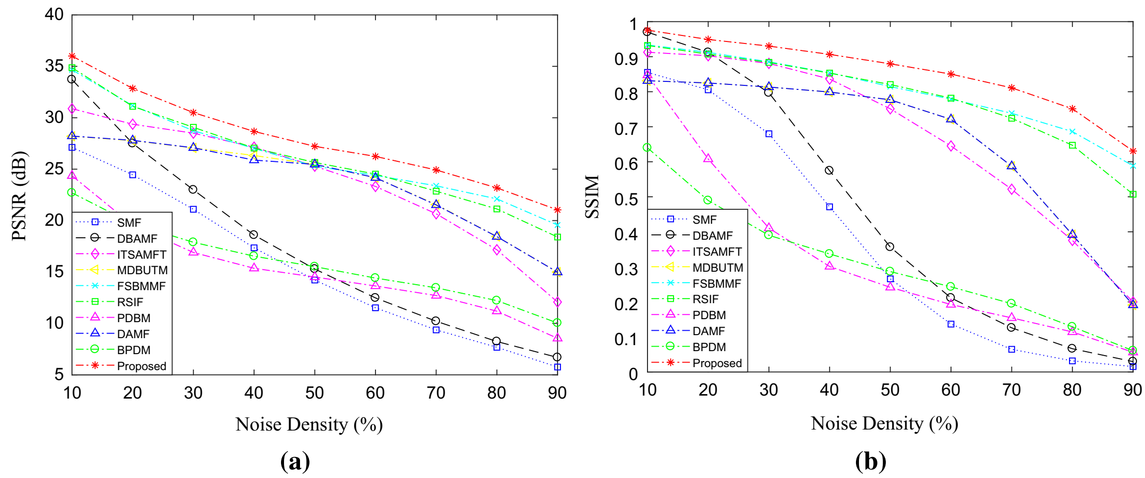

Fig. 3 Average PSNR and SSIM of filtered images using different filters for varying noise density (10–90%)

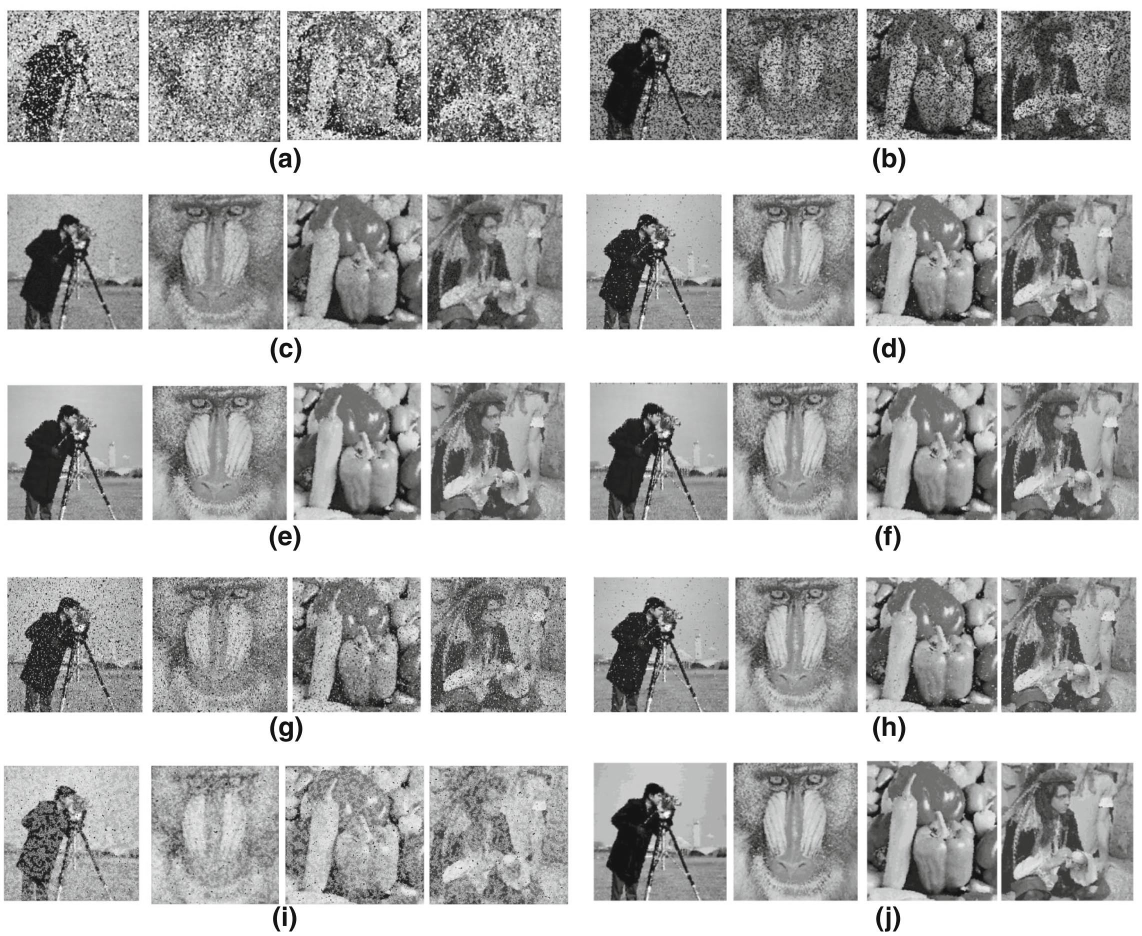

Fig. 4 Benchmark images (256 × 256) with 70% noise density filtered using: **a** SMF, **b** DBAM, **c** ITSAM, **d** MDBUTM, **e** FSBMM, **f** RSI, **g** PDBM, **h** DAMF, **i** BPDM and **j** Proposed median filters

Table 2 PSNR and SSIM of various algorithms for different color benchmark images at 90% noise density

Metrics	Benchmark	SMF	DBAM	ITSAM	MDBUTM	FSBMM	RSI	PBDM	DAMF	BPDM	ATM
PSNR	Lena	6.36	6.56	12.34	14.73	22.11	20.20	8.54	14.72	10.23	22.49
	Mandril	6.31	7.08	12.13	13.73	17.28	16.67	8.81	13.71	10.31	17.64
	Average	6.33	6.82	12.24	14.23	19.69	18.44	8.68	14.21	10.27	20.06
SSIM	Lena	0.0157	0.0350	0.2224	0.1801	0.6721	0.5850	0.0602	0.1796	0.0634	0.6928
	Mandril	0.0154	0.0414	0.1400	0.1437	0.3198	0.2840	0.0647	0.1433	0.0758	0.3344
	Average	0.0156	0.0382	0.1812	0.1619	0.4959	0.4345	0.0624	0.1614	0.0696	0.5136

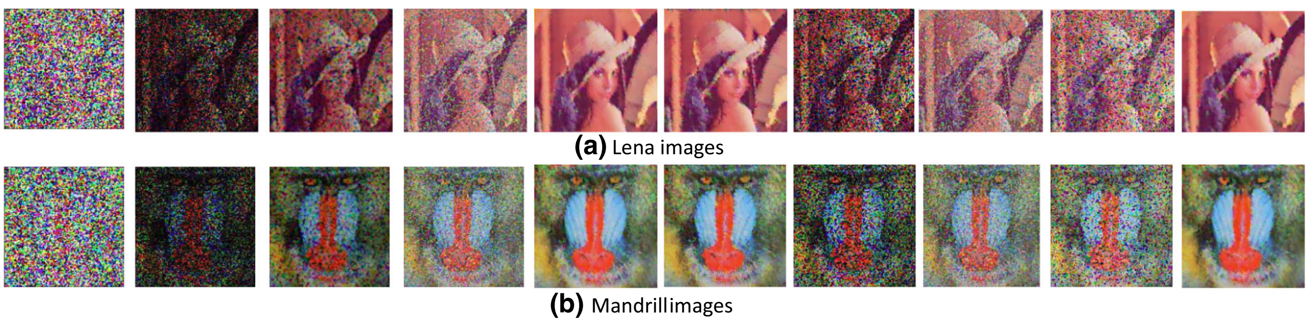

Fig. 5 Benchmark **a** Lena and **b** Mandrill images with 90% noise density filtered from left to right using SMF, DBAM, ITSAM, MDBUTM, FSBMM, RSI, PDBM, DAMF, BPDM and Proposed median filters

images. Finally, the filtered images show better visual representation over the images restored using existing algorithms even at high noise density.

References

1. Astola, J., Kuosmaneen, P.: Fundamentals of Nonlinear Digital Filtering. CRC, Boca Raton (1997)
2. Hwang, H., Haddad, R.A.: Adaptive median filters: new algorithms and results. IEEE Trans. Image Process. **4**(4), 499–502 (1995)
3. Zhang, S., Karim, M.A.: A new impulse detector for switching median filters. IEEE Signal Process. Lett. **9**(11), 360–363 (2002)
4. Ng, P.-E., Ma, K.-K.: A switching median filter with boundary discriminative noise detection for extremely corrupted images. IEEE Trans. Image Process. **15**(6), 1506–1516 (2006)
5. Deivalakshmi, S., Palanisamy, P.: Improved tolerance based selective arithmetic mean filter for detection and removal of impulse noise. In: 2010 5th International Conference on Industrial and Information Systems. IEEE, 2010, pp. 309–313
6. Srinivasan, K., Ebenezer, D.: A new fast and efficient decision-based algorithm for removal of high-density impulse noises. IEEE Signal Process. Lett. **14**(3), 189–192 (2007)
7. Ahmed, F., Das, S.: Removal of high-density salt-and-pepper noise in images with an iterative adaptive fuzzy filter using alpha-trimmed mean. IEEE Trans. Fuzzy Syst. **22**(5), 1352–1358 (2013)
8. Esakkirajan, S., Veerakumar, T., Subramanyam, A.N., PremChand, C.: Removal of high density salt and pepper noise through modified decision based unsymmetric trimmed median filter. IEEE Signal Process. Lett. **18**(5), 287–290 (2011)
9. Vasanth, K., Kumar, V.J.S.: Decision-based neighborhood-referred unsymmetrical trimmed variants filter for the removal of high-density salt-and-pepper noise in images and videos. SIViP **9**(8), 1833–1841 (2015)
10. Bhadouria, V.S., Ghoshal, D., Siddiqi, A.H.: A new approach for high density saturated impulse noise removal using decision-based coupled window median filter. SIViP **8**(1), 71–84 (2014)
11. Li, Z., Liu, G., Xu, Y., Cheng, Y.: Modified directional weighted filter for removal of salt & pepper noise. Pattern Recogn. Lett. **40**, 113–120 (2014)
12. Zhang, P., Li, F.: A new adaptive weighted mean filter for removing salt-and-pepper noise. IEEE Signal Process. Lett. **21**(10), 1280–1283 (2014)
13. Vijaykumar, V., Mari, G.S., Ebenezer, D.: Fast switching based median-mean filter for high density salt and pepper noise removal. AEU Int. J. Electron. Commun. **68**(12), 1145–1155 (2014)
14. Faragallah, O.S., Ibrahem, H.M.: Adaptive switching weighted median filter framework for suppressing salt-and-pepper noise. AEU Int. J. Electron. Commun. **70**(8), 1034–1040 (2016)
15. Veerakumar, T., Esakkirajan, S., Vennila, I.: Recursive cubic spline interpolation filter approach for the removal of high density salt-and-pepper noise. SIViP **8**(1), 159–168 (2014)
16. Li, Z., Cheng, Y., Tang, K., Xu, Y., Zhang, D.: A salt & pepper noise filter based on local and global image information. Neurocomputing **159**, 172–185 (2015)
17. Dong, Y., Xu, S.: A new directional weighted median filter for removal of random-valued impulse noise. IEEE Signal Process. Lett. **14**(3), 193–196 (2007)
18. Lu, C.-T., Chou, T.-C.: Denoising of salt-and-pepper noise corrupted image using modified directional-weighted-median filter. Pattern Recogn. Lett. **33**(10), 1287–1295 (2012)
19. Ma, H., Nie, Y.: A two-stage filter for removing salt-and-pepper noise using noise detector based on characteristic difference parameter and adaptive directional mean filter. PLoS ONE **13**(10), 1–24 (2018)
20. Ma, H., Nie, Y.: Mixed noise removal algorithm combining adaptive directional weighted mean filter and improved adaptive anisotropic diffusion model. Math. Probl. Eng. **2018**, 1–19 (2018)

21. Habib, M., Hussain, A., Rasheed, S., Ali, M.: Adaptive fuzzy inference system based directional median filter for impulse noise removal. AEU Int. J. Electr. Commun. **70**(5), 689–697 (2016)
22. Kiani, V., Zohrevand, A.: A fuzzy directional median filter for fixed-value impulse noise removal. In: 7th Iranian Joint Congress on Fuzzy and Intelligent Systems (CFIS). IEEE, vol. 2019, pp. 1–4 (2019)
23. Li, O., Shui, P.-L.: Noise-robust color edge detection using anisotropic morphological directional derivative matrix. Sig. Process. **165**, 90–103 (2019)
24. Xing, Y., Xu, J., Tan, J., Li, D., Zha, W.: Deep cnn for removal of salt and pepper noise. IET Image Proc. **13**(9), 1550–1560 (2019)
25. Fu, B., Zhao, X., Li, Y., Wang, X., Ren, Y.: A convolutional neural networks denoising approach for salt and pepper noise. Multimed. Tools Appl. **78**(21), 30 707–30 721 (2019)
26. Balasubramanian, G., Chilambuchelvan, A., Vijayan, S., Gowrison, G.: Probabilistic decision based filter to remove impulse noise using patch else trimmed median. AEU Int. J. Electr. Commun. **70**(4), 471–481 (2016)
27. Lu, C.-T., Chen, Y.-Y., Wang, L.-L., Chang, C.-F.: Removal of salt-and-pepper noise in corrupted image using three-values-weighted approach with variable-size window. Pattern Recogn. Lett. **80**, 188–199 (2016)
28. Roy, A., Laskar, R.H.: Non-casual linear prediction based adaptive filter for removal of high density impulse noise from color images. AEU Int. J. Electron. Commun. **72**, 114–124 (2017)
29. Erkan, U., ökrem, L.G., Enginoğlu, S.: Different applied median filter in salt and pepper noise. Comput. Electr. Eng. **70**, 789–798 (2018)
30. Erkan, U., ökrem, L.G.: A new method based on pixel density in salt and pepper noise removal. Turk. J. Electr. Eng. Comput. Sci. **26**(1), 162–171 (2018)
31. Wang, Z., Bovik, A.C., Sheikh, H.R., Simoncelli, E.P., et al.: Image quality assessment: from error visibility to structural similarity. IEEE Trans. Image Process. **13**(4), 600–612 (2004)